Vision Research 49 (2009) 2067–2077

Contents lists available at ScienceDirect

Vision Research

journal homepage: www.elsevier.com/locate/visres

Intraretinal processing following photoreceptor rescue by non-retinal cells ☆

I. Pinilla [a,f], N. Cuenca [b,f], G. Martínez-Navarrete [b], R.D. Lund [c,f,*], Y. Sauvé [d,e,f]

[a] Department of Ophthalmology, Hospital Universitario Miguel Servet, Zaragoza, Instituto Aragones de Ciencias de la Salud, Spain
[b] Departament of Physiology, Microbiology and Genetics, Universidad de Alicante, Alicante, Spain
[c] Department of Ophthalmology, Casey Eye Institute, Oregon Health and Science University, Portland, USA
[d] Department of Ophthalmology, University of Alberta, Edmonton, Canada
[e] Departments of Physiology, University of Alberta, Edmonton, Canada
[f] Department of Ophthalmology and Visual Science, John Moran Eye Center, University of Utah, USA

ARTICLE INFO

Article history:
Received 24 March 2009
Received in revised form 10 May 2009

Keywords:
Retinal dystrophy
RCS rats
Cell-based therapy
Photoreceptors
Electroretinogram

ABSTRACT

Royal College of Surgeon (RCS) rats undergo retinal degeneration due to the inability of retinal pigment epithelial (RPE) cells to phagocytose shed outer segments. We explored the effect of introducing Schwann cells to the subretinal space of RCS rats (before the onset of retinal degeneration), by relying on electroretinogram (ERG) recordings and correlative retinal morphology. Scotopic ERGs recorded from cell-injected eyes showed preserved amplitudes of mixed a-wave b-wave, rod b-waves, and cone b-waves over controls (sham-injected eyes); photopic b-wave amplitudes and critical flicker fusion were also improved. Normal retinal morphology was found in areas of retinas that had received cell injections. Since Schwann cells have no phagocytic properties, their therapeutic effect is best explained through a paracrine mechanism (secretion of factors that ensure photoreceptor survival).

1. Introduction

Disorders affecting RPE cell function are associated with secondary loss of photoreceptors. They include age related macular degeneration (AMD) and some forms of retinitis pigmentosa (RP) in which mutations affect RPE-related genes, such as RPE65 (Gu et al., 1997; Marlhens et al., 1997; Maw et al., 1997; Petrukhin et al., 1998) and Mertk (Gal et al., 2000; McHenry et al., 2004; Thompson et al., 2002). Cell-based therapy is one of several experimental approaches that are currently being explored for their potential to prevent retinal degeneration or even possibly restore retinal function in RP and AMD. One extensively used model is the RCS rat, which has a recessive mutation in the Mertk receptor tyrosine kinase gene (D'Cruz et al., 2000; Nandrot et al., 2000) that precludes RPE cells from phagocytosing shed rod outer segments effectively, resulting in the death of photoreceptors (Bourne, Campbell, & Tansley, 1938; Dowling & Sidman, 1962). This pathology is autologous to a human form of RP (Gal et al., 2000), and by virtue of the primary defect being in the RPE cells, it may serve as an analogous model of some aspects of AMD. A series of studies has shown that subretinal injections of cells obtained from a range of human and animal cell lines can limit rod and cone cell death in RCS rats (Arnhold et al., 2006; Gamm et al., 2007; Huang et al., 2006; Inoue et al., 2007; Lawrence et al., 2000, 2004; Lin, Fan, Sheedlo, Aschenbrenner, & Turner, 1996; Little et al., 1996; Lund et al., 2001; Lund, Wang, Klimanskaya, Holmes, & Ramos-Kelsey, 2006; Mizumoto, Mizumoto, Shatos, Klassen, & Young, 2003; Pinilla, Cuenca, Sauvé, Wang, & Lund, 2007; Rezai, Kohen, Wiedemann, & Heimann, 1997; Schraermeyer et al., 2001; Schraermeyer, Kociok, & Heimann, 1999; Seiler, Sagdullaev, Woch, Thomas, & Aramant, 2005; Thumann, Salz, Walter, & Johnen, 2009; Wang, Lu, & Lund, 2005; Wang, Lu, Wood, & Lund, 2005; Wojciechowski, Englund, Lundberg, Wictorin, & Warfvinge, 2002). Moreover, electrophysiological (Lund et al., 2001; Sauvé, Girman, Wang, Keegan, & Lund, 2002; Sauvé, Klassen, Whiteley, & Lund, 1998; Sauvé, Lu, & Lund, 2004) and psychophysical (McGill, Douglas, Lund, & Prusky, 2004; McGill, Lund, Douglas, Wang, Lu, & Prusky, 2004) assessments have shown that some level of visual function can be preserved in such treated animals. However, it remains unclear how rescue translates into respective function of rod and cone pathways.

The aim of this study was to use ERG to gain insights into intraretinal processing after Schwann cell transplantation. Schwann cells grafted subretinally, prolong photoreceptor survival in RCS rats (Lawrence et al., 2000, 2004) and in rhodopsin knockout mice (Keegan et al., 2003). Schwann cells produce several different growth factors, known when injected into the vitreous to sustain

☆ Grant information: This work was supported by FFB (Foundation Fighting Blindness), Wynn Foundation, Lincy Grant and RPB Grants. Dr. Cuenca and Dr. Pinilla were supported by a grant from the Spanish Government (BFU2006-00957/BFI, RETICS RD07/0062/0012 and Fundaluce for NC and FIS 02/5010 for IP). Dr. Sauvé is a recipient of the Barbara Tuck/MacPhee Family Vision Research Award in Macular Degeneration and an AHFMR Senior Scholar.

* Corresponding author. Address: Department of Ophthalmology, Casey Eye Institute, Oregon Health and Science University, Portland, USA.
E-mail address: lundr@ohsu.edu (R.D. Lund).

0042-6989/$ - see front matter © 2009 Elsevier Ltd. All rights reserved.
doi:10.1016/j.visres.2009.05.014

photoreceptors including CNTF (Cayouette, Behn, Sendtner, Lachapelle, & Gravel, 1998; Sendtner, Stöckli, & Thoenen, 1992), BDNF (Meyer, Matsuoka, Wetmore, Olson, & Thoenen, 1992), GDNF (Hammarberg et al., 1996) and bFGF (Neuberger & De Vries, 1993). Therefore, we relied on subretinal human Schwann cell (hSC) injections as a mean to examine how preservation of photoreceptors, using such a continuous growth factor delivery approach, might impact on rod and cone-driven retinal function and on their respective retinal circuitry. Our findings indicate that while subretinal injections of hSCs can partially preserve both rod and cone ERG function, retina responsiveness remains abnormal, more so for rod than cone-driven pathways; furthermore, there are signs of decline in effectiveness with postoperative time. Defective phototransduction as well as post-synaptic processing (of a biochemical nature rather than noticeable morphological remodeling) might account for the progressive decline in retina responsiveness (as assessed with the ERG) over post-cell therapy intervention; immune considerations must also be addressed in further studies.

2. Experimental procedures

2.1. Animals

This work was done in a dedicated cohort of dystrophic (RCS rdy+ p+, $n = 21$) and non-dystrophic congenic (RCS rdy− p+, $n = 9$) pigmented RCS rats, which were bred in a colony at the University of Utah, and maintained under a 12 h light/dark cycle (light cycle mean illumination: 30 cd/m^2). All animals were housed and handled with the authorization and supervision of the Institutional Animal Care and Use Committee from the University of Utah. Every procedure conformed to the National Institute of Health Guide for the Care and Use of Laboratory Animals (NIH Publications No. 80-23) revised 1996. The procedures also conformed to the ARVO Statement for the Use of Animals in Ophthalmic and Vision Research.

2.2. Preventive subretinal transplantation

At age P21–23, dystrophic RCS rats received subretinal injections of a suspension of human Schwann cells as previously described (Wang et al., 2005). In brief, following anesthesia with xylazine–ketamine (1 mg/kg i.p. of the following mixture: 2.5 ml xylazine at 20 mg/ml, 5 ml ketamine at 100 mg/ml, and 0.5 ml distilled water), dystrophic RCS rats received subretinal injections of cells ($n = 12$) or medium alone ($n = 9$). All injections were made in the upper temporal retina of the right eye: the left eye served as the untreated control. Cultures of human Schwann cells were trypsinized, washed and delivered as a suspension (2×10^5 cells per injection) in 2 μl of Ham's F10 medium through a fine glass pipette (internal diameter 75–150 μm) into the eye via a tiny scleral incision (Sauvé et al., 2002). All animals received daily dexamethasone injections (1.6 mg/kg, i.p.) for 2 weeks and were maintained on cyclosporine administered in the drinking water (210 mg/l; resulting blood concentration: 250–300 μg/l; Coffey et al., 2002) from 2 to 3 days prior transplantation until sacrifice.

2.3. ERG recordings

Animals were prepared under dim red light following overnight dark adaptation, and ERGs recorded as previously described (Pinilla, Sauvé, & Lund, 2004; Sauvé, Pinilla, & Lund, 2006). At P60, ERGs were recorded from three congenics, the 12 hSC-injected animals and the nine sham-injected animals; after which four of the hSC-injected animals and all nine shams were culled and used for anatomy. At P90, two additional congenics and the eight remaining hSC-injected animals were recorded again for ERGs.

2.4. Mixed scotopic ERG responses

Recordings consisted of 3–5 single flash presentations (standard duration of 10 μs). Stimuli were presented at sixteen increasing intensities varying from −3.7 to 2.86 log cds/m^2 in luminance. To minimize rod bleaching inter-stimuli-intervals (ISI) were increased as the stimulus luminance was elevated from 10 s at the lowest stimulus intensity up to 2 min at the highest stimulus intensity. The maximal b-wave amplitude was that obtained during the flash intensity series, regardless of the specific stimulus intensity. Criterion amplitudes were established at 10 μV for a-waves and b-waves.

2.5. Isolation of scotopic rod and cone responses using a double flash protocol

A double flash protocol as previously described (Pinilla et al., 2004; Sauvé et al., 2006), was used to isolate rod and cone ERG components. A probe flash was presented 1 s after a conditioning flash (1.4 log cds/m^2). Response to this flash was taken as reflecting cone-driven activity. A rod-driven b-wave was obtained by subtracting the cone-driven response from the mixed response (obtained following presentation of a probe flash alone).

Averages of up to three traces were used: intervals between double flash presentations were set at 2 min to assure full recovery of rod responsiveness. Control studies confirmed the validity of the experimental conditions.

2.6. Photopic ERG responses

After completion of ERG recordings under scotopic adaptation, rats were light adapted for 20 min with a background illumination of 30 cd/m^2 to reach a stable photopic response level. Photopic intensity responses (30 cd/m^2 background) consisted of six increasing intensities ranging from −1.6 to 2.9 log cds/m^2. Flicker responses were recorded to white strobe flash presentations in a ganzfeld stimulator with a luminance of 31.5 log cd/m^2. Flash intensity was set to 1.4 log cds/ m^2. Stimuli were presented at 3 Hz, and then at 5 Hz up to 50 Hz in 5 Hz steps. When flicker fusion was achieved (criterion amplitude of 3 μV), lower frequencies were studied; 40 responses were averaged at each frequency tested.

2.7. Recovery from conditioning flash

Finally, we examined the recovery phase of the b-wave following bleaching with a conditioning flash (1.4 log cds/m^2). This was achieved by recording the responses to a test flash (1.4 log cds/ m^2) presented at increasing intervals following the presentation of the conditioning flash. Experiments were done under scotopic adaptation (as the last scotopic tests) and repeated following photopic adaptation (after photopic intensity response, prior to flicker testing). The delays studied consisted of: 30, 60, 120, 240, 480, 960, 2000, 4000 and 8000 ms.

2.8. Statistics

Errors are expressed as standard errors of the mean (SEM). Comparisons between two different groups were made using Mann–Whitney *U*-test. The probability level was set at $p < 0.05$.

2.9. Immunohistochemistry

Histological evaluation was done for hSC-injected eyes ($n = 4$) and sham-injected eyes ($n = 4$) at ages P70. Following ERG recordings, animals were overdosed with urethane (12.5 g/kg i.p.; ten times higher than the normal anesthetic dose) and perfused tran-

Table 1
Antibodies used in the present study.

Antigen	Antiserum	Source	Dilution
Bassoon	Mouse anti-bassoon	Stressgen	1:5000
Calbindin	Rabbit anti-CB	Swant	1:500
Caldindin	Mouse anti-CB	Sigma	1:500
Metabotropic glutamate receptor 6	Rabbit anti-mGluR6	Neuromics	1:3000
Protein kinase C	Rabbit anti-PKC	Santa Cruz	1:100
Protein kinase C	Mouse anti-PKC	Santa Cruz	1:100
Recoverin	Mouse anti-recoverin	Dr. McGinnis	1:5000
Recoverin	Rabbit anti-recoverin	Dr. McGinnis	1:20,000
γ-Transducin	Rabbit anti-γ-transducin	Cytosignal	1:500

scardially with phosphate buffered saline (PBS). Both eyes were enucleated. The immunohistochemistry protocol was the same as previously described (Cuenca et al., 2004). The primary antibodies used in this study are presented in Table 1. Sections were viewed using confocal microscopy (Leica TCS SP2).

3. Results

3.1. Non-dystrophic RCS rats

Three congenic animals were examined at age P60 ($n = 3$) and P90 ($n = 2$) to provide normative data. Since no statistical differences were found between the two time points, all data were pooled for analysis ($n = 5$). Thresholds for scotopic a-waves were at -2.44 log cds/m^2. The amplitude of the a-wave increased with stimulus intensity and reached maximal values (599 ± 73 μV at) at 2.39 log cds/m^2, the penultimate intensity tested. At the lowest intensity tested (-3.70 log cds/m^2), the b-wave already had amplitudes of 214 ± 52 μV, and peaked to 1214 ± 57 μV at 1.89 log cds/m^2 with no decrements at higher amplitudes. Double flash-derived rod b-waves had similar thresholds as mixed b-waves, indicating pure rod responses at these low levels: amplitudes increased proportionally to stimulus intensity, peaking to 987 ± 64 μV at 1.89 log cds/m^2. Both isolated scotopic cone b-waves and photopic b-waves showed a similar variation in amplitude with stimulus intensity. B-wave amplitudes reached a plateau at 0.38 log cds/m^2. However thresholds were lower and maximal amplitudes larger under scotopic conditions. With regard to flicker ERG, an approximately linear relationship was observed when plotting the log response amplitude against the flicker frequency. The function that best fitted this relationship was of the exponential type: $y = ce^{bx}$; giving a coefficient of correlation R^2 of 0.9814. Flicker amplitudes were maximal (332 ± 183 μV) at 3 Hz, the lowest frequency tested and fused at 40.9 Hz. Initial recovery of mixed b-waves from the conditioning flash was accomplished at 120 ms and full recovery (amplitudes reaching normalized values of one) required more than 10 s: corresponding values for photopic b-waves were at 60 ms for initial recovery and 120 ms for full recovery.

3.2. Dystrophic RCS rats

3.2.1. Sham-injected eyes

Previous studies (Sauvé et al., 2004, 2006) have shown that ERG responses in sham-injected eyes are comparable to those recorded in untreated dystrophic eyes. That is, already by P60, a-waves can no longer be elicited and b-waves just barely reach criterion levels, vanishing by P90. All average data for sham-injected eyes are represented as unfilled circles.

3.2.1.1. Mixed scotopic responses. ERG tests applied at P60 (using conventional single flash presentation at various intensities, under scotopic adaptation) demonstrate that hSC injections lead to the preservation of both mixed a- and b-waves when compared with sham injections. Fig. 1 shows intensity versus response curves as average data (±SEM) for all animals studied at all time points.

While no a-wave could be recorded in sham-injected eyes at P60, hSC-injected eyes retained a-waves up to P90 (Fig. 1). At P60, a-wave thresholds were at -0.41 log cds/m^2. The amplitude of the a-wave increased with stimulus intensity reaching maximal values (47.3 ± 13.6 μV) at 2.85 log cds/m^2. By P90, a-wave thresholds increased to -1.36, and the maximum a-wave amplitude was still achieved using the highest stimulus intensity (2.85 log cds/m^2).

The center column of Fig. 1 shows intensity response curves for mixed b-waves. At P60, b-wave amplitudes were higher throughout the whole range of intensities tested with the exception of the lowest level (-3.7 log cds/m^2), the maximum amplitude (186 ± 11.3 μV) far exceeding the best response in sham-injected

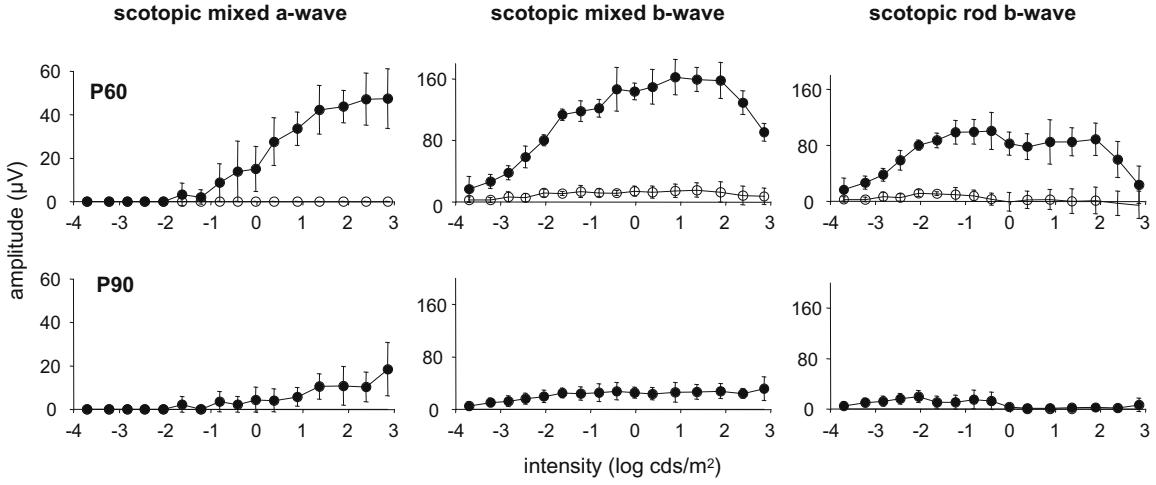

Fig. 1. ERG amplitude versus flash intensity (*V*-log I) series of mixed a-waves (left column), mixed b-waves (center column) and double flash isolated rod b-waves (right column) for animals recorded longitudinally at ages P60 and P90 (presented along respective rows). Filled circles: hSC-injected eyes (P60 $n = 12$, P90 $n = 8$); unfilled circles: sham-injected eyes ($n = 9$). Statistically significant higher amplitudes were seen for all ERG components when comparing results from hSC-injected with those from sham-injected eyes at age P60. Sham-injected eyes were recorded at P60 only. Statistically significant higher amplitudes were still seen for all components when comparing results from hSC-injected eyes at P90 ($n = 8$) with those from sham-injected eyes at P60 ($n = 9$). Note the drop in maximal amplitude (for all components) between P60 and P90 in hSC-injected eyes. Error bars = SEM.

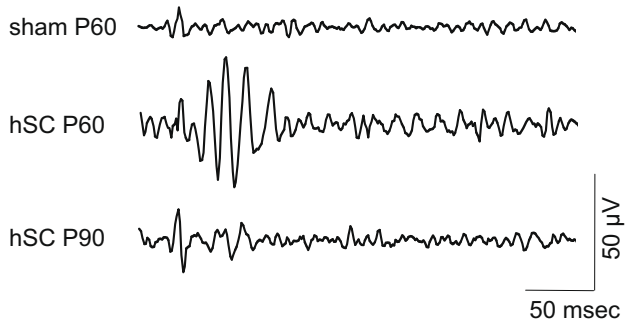

Fig. 2. Examples of oscillatory potentials elicited by a 1.37 log cds/m^2 flash under scotopic conditions. Injection of hSC cells resulted in preserved oscillatory potentials at P60 but not after. Note the absence of oscillatory potentials in the sham-injected eye at P60.

eyes (15.2 ± 9.3 μV). At −3.2 log cds/m^2, b-waves surpassed the criterion level of 10 μV only in hSC-injected eyes, and at all ages b-waves could still be elicited in hSC-injected eyes at this intensity. B-wave amplitudes increased as a function of stimulus intensity, then reached a plateau (with maximal intensity at −0.88 log cds/m^2), and finally decreased progressively, with values getting significantly lower (than values reached at the plateau) at the two highest intensities tested (2.39 and 2.86 log cds/m^2). Oscillatory potentials (OPs) had significantly higher amplitudes in hSC-injected eyes in comparison to sham-injected eyes: average amplitude at 1.37 log cds/m^2 of 140.6 ± 14.1 μV versus 16.25 ± 5.8 μV, respectively (Fig. 2). With age, after P60, OP amplitudes were severely diminished in hSC-injected eyes and maximal mixed b-wave amplitudes reached a plateau at lower luminance intensities (35.5 ± 10.5 μV at −1.22 log cds/m^2 for P90). Isolated rod scotopic responses.

Using a double-flash protocol (Pinilla et al., 2004), we dissected both rod and cone contributions to the mixed scotopic b-wave. Fig. 1 shows averages of intensity response curves for double flash isolated rod b-waves. At P60, rod-driven responses were significantly higher in hSC-injected eyes (maximum of 90.33 ± 9.8 μV) than in sham-injected eyes (maximum of 25.3 ± 3.5 μV) and persisted at P90, with an average maximal value of 37.7 ± 13.8 μV. At P60, when compared to the mixed scotopic b-waves, isolated rod b-waves reached maximal amplitudes at lower stimulus intensities (67.1 ± 9.8 μV at 2.86 log cds/m^2 compared with 74.3 ± 4.4 μV maximal value reached at 1.3 log cds/m^2) using 2 min ISI. In two animals, we extended the interstimulus interval up to 10 min and achieved a maximum response of 70.8 ± 9.8 μV.

The intensity at which maximal rod b-wave amplitudes were reached remained the same independently of age in hSC-injected animals. In all sham-injected animals, as the intensity of the stimulus increased, b-waves were progressively replaced by negative going components, analogous to the high threshold scotopic threshold responses (STR) previously reported in RCS rats (Bush, Hawk, & Sieving, 1995; Sauvé et al., 2006). Such STR-like responses were not seen in hSC-injected animals. Double flash isolated scotopic cone responses.

The ERG results show that subretinal injections of hSC cells are associated with the preservation of cone-driven responses when compared with sham injections. Fig. 3 shows averages of intensity response curves for double flash isolated scotopic cone b-waves. At P60, b-wave thresholds were lower for hSC-injected eyes (−1.63 log cds/m^2) compared with shams (−0.42 log cds/m^2). B-wave amplitudes were significantly higher in hSC-injected eyes (maximum of 90.3 ± 9.9 μV) compared with shams (maximum of 25.3 ± 3.6 μV) and were still present at P90, with an average maximal value of 42.5 ± 7.5 μV. Amplitudes increased with stimulus intensity, peaking at 1.37 log cds/m^2 in hSC-injected eyes but at a much lower level (−0.02 log cds/m^2) in sham-injected eyes. However, from P60 to P90, there was a significant decrease in maximal b-wave amplitude in hSC-injected eyes and plateaus were reached at lower stimulus intensities, as was the case in sham-injected eyes at P60.

3.2.1.2. Single flash photopic responses. Photopic intensity responses (Fig. 3) were of lower amplitudes than double flash isolated scotopic cone responses. Intensity response curves for photopic b-waves are presented in Fig. 3. At P60, b-wave thresholds for hSC-injected eyes were achieved at −0.81 log cds/m^2; the lowest threshold in sham-injected eyes was −0.41 cds/m^2, and this was only seen in one animal. B-wave amplitudes increased with stimulus intensity, peaking at 0.88 log cds/m^2 in hSC-injected eyes. B-wave amplitudes were significantly higher in hSC-injected eyes (maximum of 66.2 ± 9.9 μV) compared with sham-injected eyes (maximum

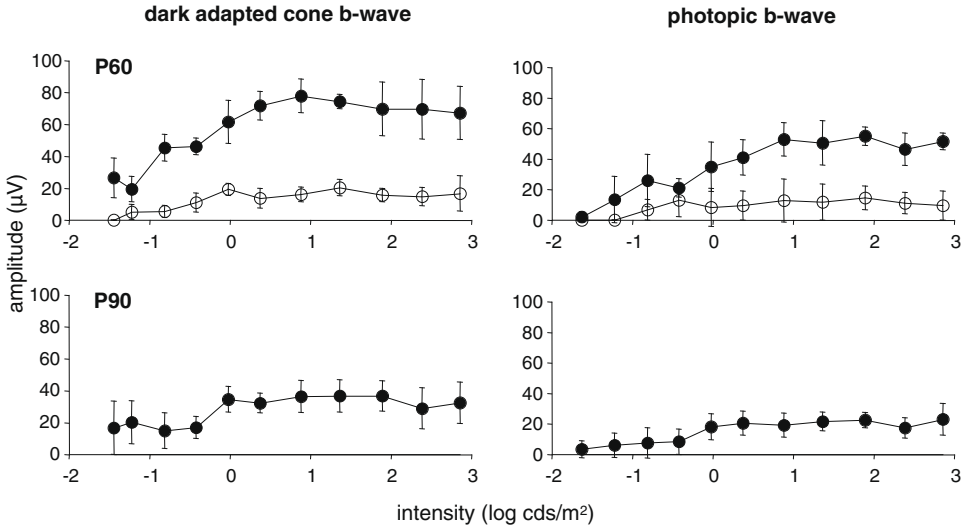

Fig. 3. ERG b-wave amplitude versus flash intensity (V−log I) series of double flash isolated scotopic cone responses (left column) and photopic responses (right column) for animals recorded longitudinally at ages P60 and P90 (presented along respective rows). Black circles: hSC-injected eyes (n = 10); white circles: sham eyes (n = 6). Statistically significant higher amplitudes were seen for all ERG components when comparing results from hSC-injected with those from sham-injected eyes at age P60. Sham-injected eyes were recorded at P60 only. Amplitudes obtained at P90 were not different for hSC-injected eyes when compared with those from sham-injected eyes at P60 (n = 6). Error bars = SEM.

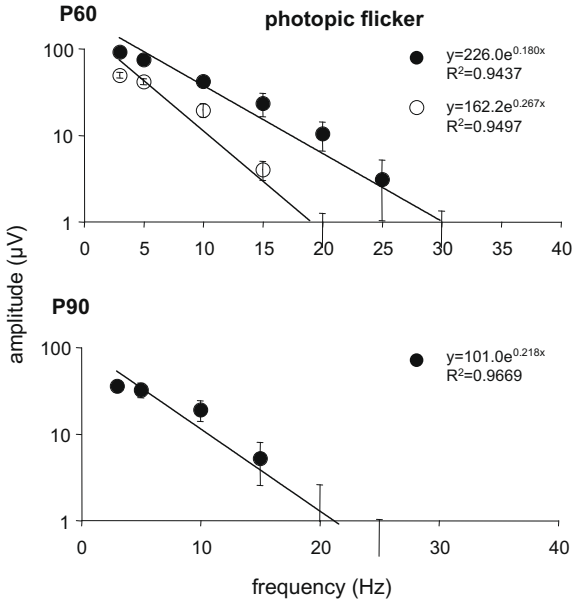

Fig. 4. Amplitude of the flicker ERG response as a function of stimulus frequency. Black circles: hSC-injected eyes (P60 $n = 12$, P90 $n = 8$); white circles: sham-injected eyes (P60, $n = 6$). Statistically significant higher amplitudes were seen for all ERG components when comparing results from hSC-injected with those from sham-injected eyes at age P60. Sham-injected eyes were recorded at P60 only. Note that due to the use of log units on the ordinates, differences between individual data points are greater than they appear; this is especially true for higher values. The equations describing the curves fitting each data set are given adjacent to each curve; values of R^2 are given under each corresponding equation. Error bars = SEM.

of 17.3 ± 11.9 μV) and persisted up to P90 although clearly diminished, with an average maximal value of 28.8 ± 6.5 μV.

3.2.2. Photopic flicker response

Flicker ERG was used to further characterize cone function. Recording from both hSC- and sham-injected RCS rat eyes showed no evidence of response fatigue over time. In all animals, at all ages, response amplitudes were maximal at the 3 Hz frequency and progressively decreased with presentation of higher frequency stimuli.

Fig. 4 shows the log response amplitude against the flicker frequency. The values of R^2 varied from 0.94 to 0.97. The constant "*c*" (corresponding to the extrapolated amplitude value at the ordinate origin) was higher in hSC-injected animals (226 ± 16) compared with sham-injected animals (162.2 ± 21) at P60, but decreased with age in hSC-injected animals (101 ± 19 at P90). The slope of this curve (related to the variable "*b*") was steeper in sham-injected (−0.267 ± 0.05) compared to hSC−injected animals (−0.180 ± 0.03). Critical flicker fusion frequencies were higher in hSC-injected (28.3 ± 2.2 Hz) than in sham-injected eyes (17.5 ± 2.5 Hz) at P60. The critical flicker fusion frequencies steeply dropped at P90 (19.5 ± 3.0 Hz) in hSC-injected eyes.

3.2.2.1. Dynamic of recovery from a conditioning flash. When tested at P60, recovery from a conditioning flash was much faster in sham-injected compared to hSC-injected eyes, both under scotopic and photopic adaptation (Fig. 5). Under scotopic conditions, sham-injected animals showed first signs of appearance of a b-wave (3 μV criterion amplitude) at 30 ms and full recovery (matching or exceeding the amplitude obtained to a single flash) already at 60 ms. In age-matched hSC-injected animals, first signs of a b-wave were only achieved at 10,000 ms with no instances of full recovery by that time. In sham-injected eyes, the levels obtained following a conditioning flash actually transiently exceeded by up to five-fold the levels achieved with a single flash. It should be noted that these amplitudes (produced by a single flash) were considerably lower in sham-injected than in hSC-injected eyes. In hSC-injected eyes, the amplitude levels at various times, following presentation of the conditioning flash, never exceeded the value of one at P60, and up to the normalized value of 2 at P90. In all cases, the optimal values of b-wave amplitudes were reached at 120 ms delay following the conditioning flash.

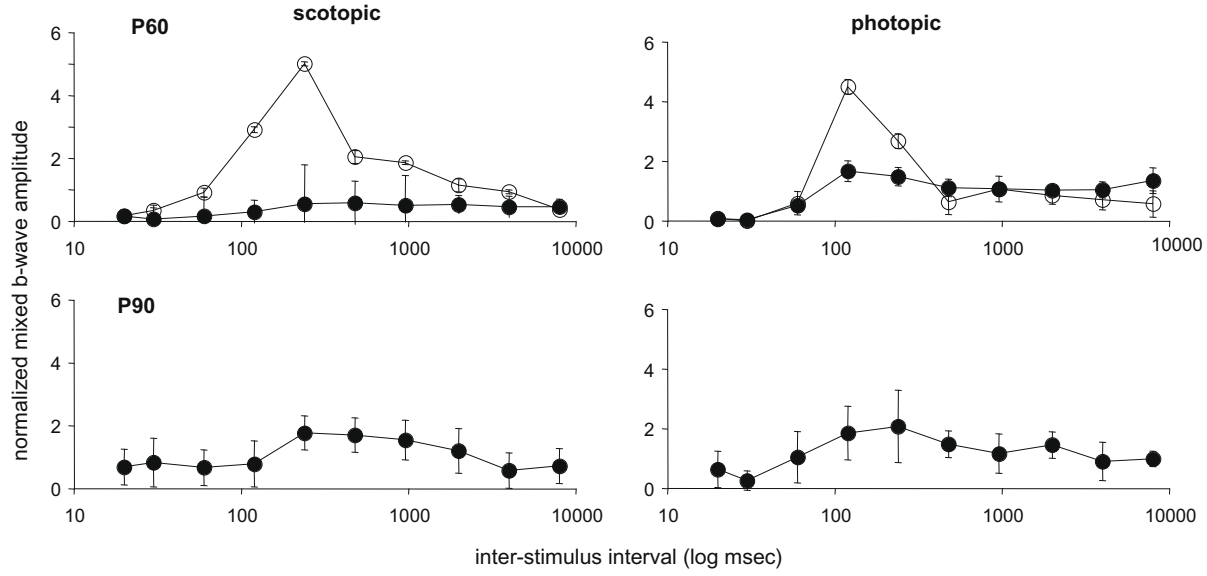

Fig. 5. Time course of b-wave recovery from a conditioning flash. The *Y*-axis represents the ratio of b-wave amplitude in response to a probe flash (second flash) versus to a conditioning flash (first flash) and the *X*-axis corresponds to the delay (in log units) between both flashes. Graphs on the left are for mixed scotopic b-waves and right-hand graphs are for photopic b-waves. Black circles: hSC-injected eyes (P60 $n = 12$, P90 $n = 8$); white circles: sham-injected eyes (P60 $n = 6$). Note, at P60, the overshoot in normalized amplitudes (exceeding amplitudes of responses to a probe flash alone) exacerbated in sham-injected eyes and the faster b-wave recovery time for the hSC-injected (60 ms) versus the sham-injected (240 ms) eye. Also, note the prolongation in b-wave recovery time for the hSC-injected eye between P60 (60 ms) and P90 (240 ms). Under photopic adaptation (30 cd/m^2), note, at P60, the faster b-wave recovery time for the hSC-injected (30 ms) versus the sham-injected (60 ms) eye. Also, note the prolongation in b-wave recovery time for the hSC-injected eye between P60 (30 ms) and P90 (60 ms). Error bars = SEM.

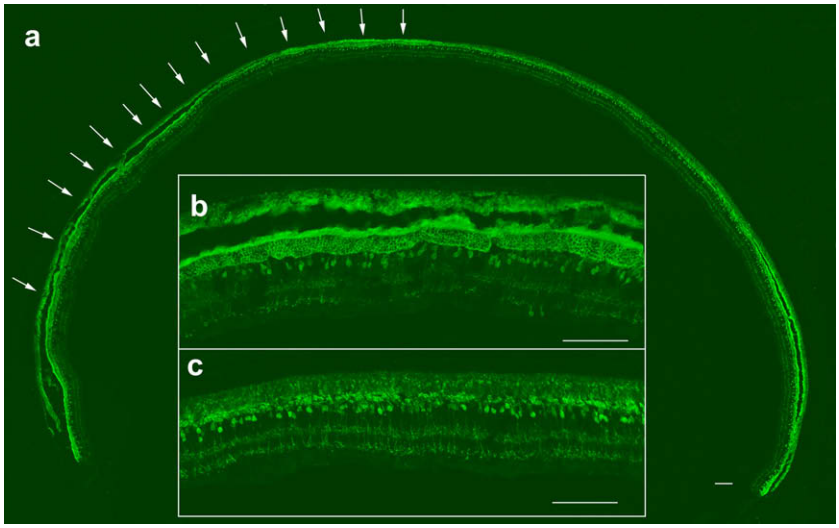

Fig. 6. Low magnification cross section of an hSC-injected eye at P70 immunolabeled with antibodies against recoverin (a). An extended area of preserved photoreceptors could be seen around the injection site (a, arrows), reaching 5–6 photoreceptor rows (inset b); these photoreceptors had well developed outer segments. The number of photoreceptors diminished toward the periphery, remaining only 1–2 cell rows (inset c). Scale bar represents 100 μm.

3.2.2.2. Histological findings. A series of previous studies (Cuenca, Pinilla, Sauvé, & Lund, 2005; Pinilla et al., 2007; Wang et al., 2005) provide the background for the present observation. In those we described the findings in normal congenic RCS rats and in dystrophic RCS rats with and without subretinal injections of RPE cell lines.

3.2.3. Photoreceptors and bipolar cells

Fig. 6a shows a cross section of a retina in which Schwann cells were injected subretinally. There was an extended area (Fig. 6a arrows) around the injection site where the outer nuclear layer was as much as 5–6 cells deep (Figs. 6b and 7a, c), compared with 12–14 layers in non-dystrophic rats (Cuenca et al., 2005; Pinilla et al., 2007). The ONL was reduced towards the periphery, to as few as 1–2 cells deep (Figs. 6c and 7b, d), similarly to that found in age-matched untreated dystrophic RCS rats (data not shown).

Photoreceptors stained with antibody against recoverin (Fig. 7a, red channel) had well developed outer segments in the area around the injection site but these segments were shorter that in normal congenic rats. Cones stained with antibody against gamma-transducin, (Fig. 7c, green channel) did not have their cell bodies confined to the outer part of the ONL, as would normally be the case, and their axon and outer segment were both shorter (Fig. 7c). In non-preserved areas, cell morphology was noticeably abnormal (Fig. 7d).

Rod bipolar cells (stained with antibody against PKC, green channel) had normal dendrites in the preserved areas (Figs. 7a and 8a). The types of cone bipolar cells stained with recoverin antibody (red) and transducin antibody (green), showed normal dendrites too (Fig. 7c). In the areas where photoreceptors were no longer preserved, cone bipolar cell bodies and axon terminals did not show appreciable changes, but rod bipolar dendrites had sprouted into the debris zone; some rod bipolar cell dendrites had abnormal morphology and other rod bipolar cells were devoid of any dendrites. Some of the cell bodies had abnormal orientations, changing their longer axis to a horizontal position (Fig. 8b).

3.2.4. Synaptic markers in the outer plexiform layer

In order to study the outer plexiform layer (OPL), we relied on two presynaptic markers against bassoon and synaptophysin and the postsynaptic marker of all ON-bipolar cells, the metabotropic glutamate receptor 6 antibody, mGluR6.

As described in previous papers (Cuenca et al., 2005), in normal rats, two types of pairings could be seen between bassoon and mGluR6: paired punctate staining profiles in the outer OPL corresponding to rod spherules, stained with bassoon, partnered with the dendritic tips of their rod bipolar cells stained with mGluR6 or with synaptic profiles appearing as disk-like formations (also stained with mGluR6), located at the inner OPL, corresponding to ON-cone bipolar cells receiving input from cone pedicles. In the transplant areas, pairs between bassoon and mGluR6 were easy to recognize (Fig. 8c, 8e). In areas remote from the injected cell area, it was unusual to find any such pairings; both bassoon and mGluR6 immunoreactivity was clearly diminished (Fig. 8d and f). Sham-injected animals at P70 showed a few spared pairings, but these did not form a continuous layer (data not shown).

3.2.5. Horizontal cells

Horizontal cells were stained using antibodies against calbindin (Fig. 9a–c). To examine whether horizontal cells maintained contacts with photoreceptor terminals, we relied on double staining with synaptophysin as a presynaptic marker (Fig. 9c, red channel) combined with calbindin (Fig. 9c). Synaptophysin stained the whole presynaptic terminal (Fig. 9c). In preserved areas, horizontal cell terminal tips were well preserved (Fig. 9a arrows): they were associated with a continuous layer of synaptophysin (Fig. 9c). In the areas remote from the injection site, horizontal cells had less numerous terminals (Fig. 9b arrows) and the synaptophysin layer had gaps with no immunoreactivity; horizontal cell tips were not always associated to their presynaptic marker (Fig. 9d).

4. Discussion

Using the RCS rat as a model of progressive photoreceptor degeneration (caused by compromised RPE function), the ERG results presented in this study indicate that subretinal injections of hSC cells can sustain both rod- and cone-driven responsiveness. However the ERG recordings show signs of dysfunction, more so for rod than cone-driven responses, and point to a steep decline in functional preservation over postoperative time; this occurs despite the anatomical persistence of photoreceptors and preserved cone function using other tests, including light and dark-adaptation studies (Girman, Wang, & Lund, 2005; Sauvé et al., 2006).

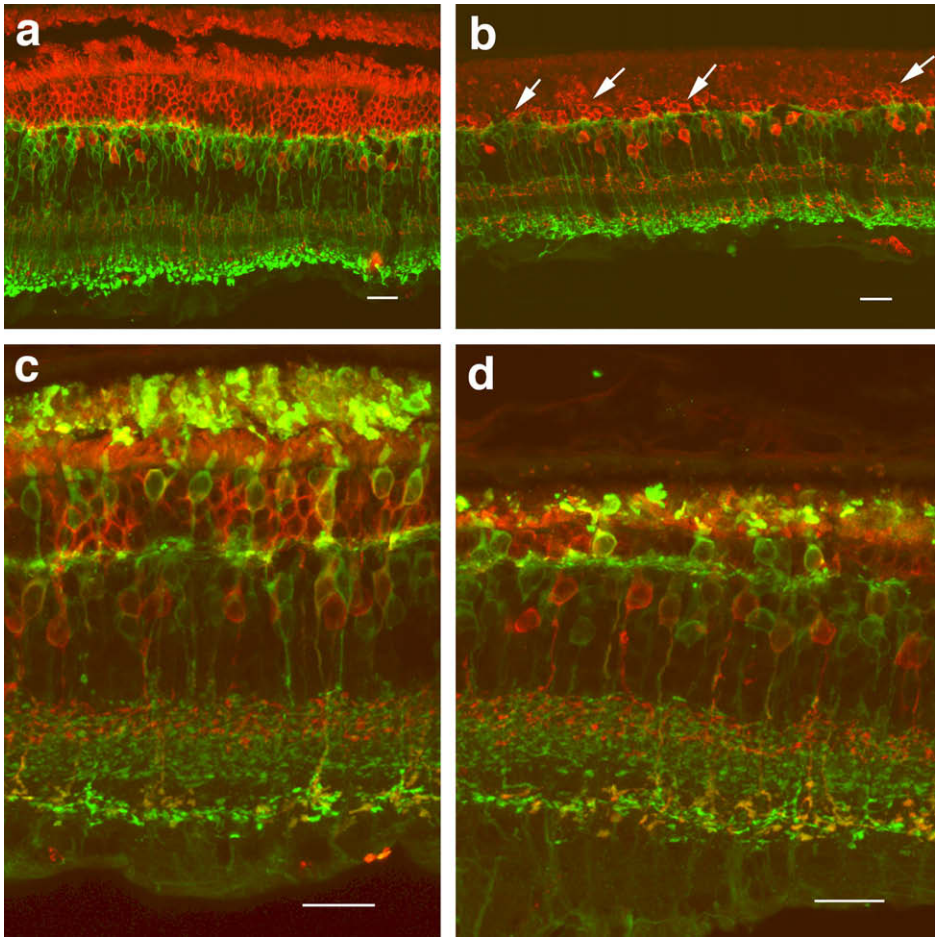

Fig. 7. Cross-retina sections showing photoreceptors and bipolar cells. (a and b) Double immunostaining with antibodies against recoverin (red) and PKC-α (green) in the area preserved by the human Schwann cell injection and away from the injection site, respectively. Photoreceptor numbers went up to 5–6 rows in transplant area (a), with only 1–2 rows far away from the transplant (b, arrows). (c and d) Double immunostaining with antibodies against recoverin (red) and α-transducin (green). In the transplant area (c), cones displayed a well-preserved morphology with shorter axon and outer segments. Cone morphology differed in non-preserved areas (d), with smaller outer segment and an increase in transducin immunoreactivity. Scale bar represents 20 μm. (For interpretation of the references to colour in this figure legend, the reader is referred to the web version of this article.)

RPE dysfunction in RCS rats first leads to the lost of rods while cone death is protracted (Dowling & Sidman, 1962; LaVail, Sidman, & Gerhardt, 1975). The first pathological changes reported in pigmented RCS rats consist of disorganized rod outer segments already by P15 (Davidorf et al., 1991) and abnormal phototransduction related to a defect in arrestin at P17 (Mirshahi, Thillaye, Tarraf, de Kozak, & Faure, 1994). Evidence of an early defect in rod phototransduction comes from immunohistochemical studies showing abnormal rhodopsin turnover already by P21 (Ohguro, Ohguro, Mamiya, Maeda, & Nakazawa, 2003). Using antibodies to the phosphorylated form of rhodopsin, Ohguro et al. (2003) found that during dark adaptation, dephosphorylation of rhodopsin was dramatically prolonged in RCS rats already at P21, taking 4–7 days to reach the low levels seen within 2 h in non-dystrophic rats. By P32–35, there is a clear diminution in the number of photoreceptors (Peng, Senda, Hao, Matsuno, & Wong, 2003) and by P90, the outer nuclear layer consists of a single cell layer made up essentially of cones, which are the last type of photoreceptors to persist in late degenerative stages (Cotter & Noell, 1984; LaVail, Sidman, Rausin, & Sidman, 1974). We have found in previous work that photoreceptor loss is accompanied by pathological changes, involving abnormal distribution of synaptic markers in the OPL, sprouting of bipolar and horizontal process as well as abnormal patterning of amacrine cell processes (Cuenca et al., 2005). Such findings were confirmed here in areas of the retinal distant from that in which photoreceptors were protected by the injected cells.

At the functional level, studies involving double flash scotopic ERGs (Pinilla et al., 2004) and light adaptation of multi-unit responses recorded from the superior colliculus (Girman et al., 2005) indicate that rod function is already deteriorated by P21 in RCS rats. In contrast to rods, cone function in RCS rats does reach maturation levels at P30 but then declines rapidly afterwards (Pinilla, Sauvé, & Lund, 2005). Perimetry-like studies involving superior colliculus recordings under mesopic adaptation indicate a loss in sensitivity first detected at P28 with a rapid decline during the next 120 days in RCS rats (Sauvé, Girman, Wang, Lawrence, & Lund, 2001). Behavioral estimates of visual acuity, under conditions that saturate rods, show a decline starting at P30 with steep loss over the next 90 days (McGill et al., 2004). The last signs of ERG responsiveness are at P180 (Pinilla et al., 2004) and consist of a slow negative deflection reminiscent of the scotopic threshold response (STR), which has been associated with inner retinal activity, most likely from retinal ganglion cells (RGCs) (Bush et al., 1995). It is unclear whether this activity is associated with RGCs that have intrinsic capability for phototransduction (Hattar, Liao, Takao, Berson, & Yau, 2002) and/or from vestigial light responsiveness still taking place in the few remaining photoreceptors whose efficacy could be enhanced in driving RGCs by retinal circuitry

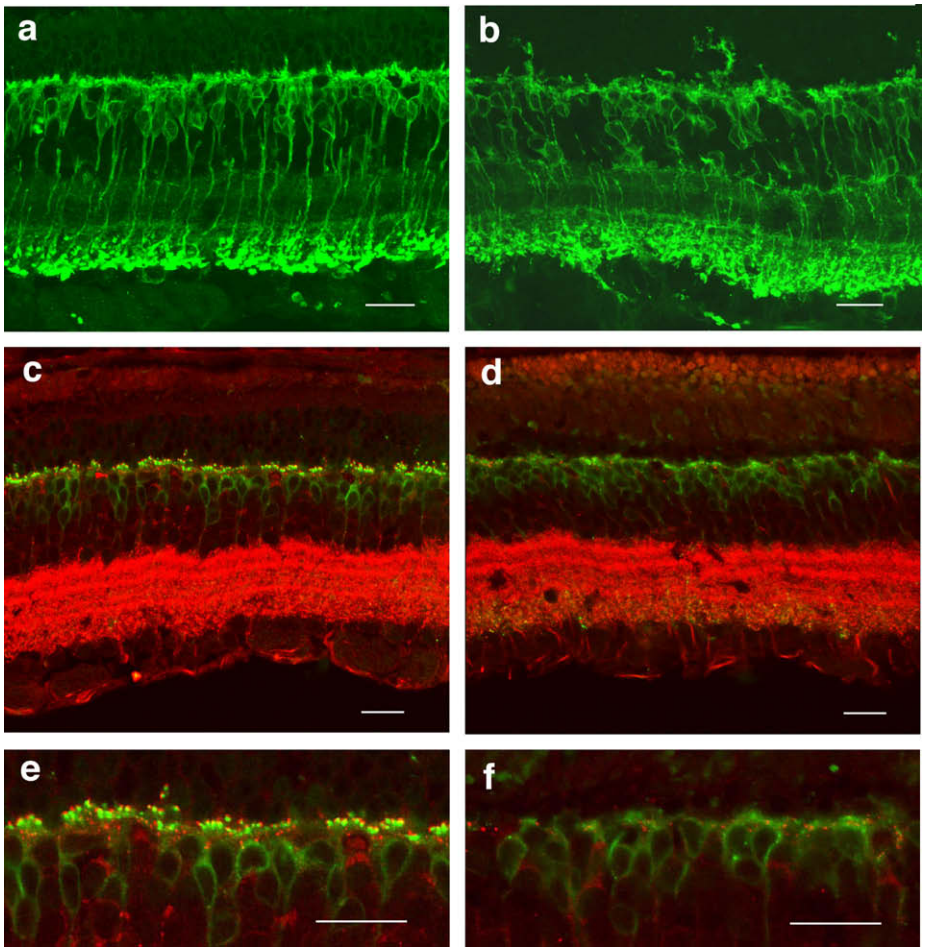

Fig. 8. Cross-retina sections showing rod bipolar cells and OPL preservation after human Schwann cells injections. (a and b) PKC-α immunostaining to study rod bipolar cells (green). Their dendrites were well developed in the preserved areas with no significant sprouting (a). Rod bipolar cells remote from the preserved areas showed dendritic sprouting into the debris zone (b). (c–f) Bassoon (red channel) staining of photoreceptor ribbon synapses and mGluR6 (green channel) staining of postsynaptic receptors of the dendritic tips of the ON-bipolar cells. (c and e) In preserved areas, bassoon-mGluR6 pairings formed a continuous layer with a punctuate profile in the outermost part of the OPL. (d and f) Remote from the preserved area, the bassoon and mGluR6 immunoreactivity was clearly diminished and it was unusual to see any pairings. In sham animals, synaptic pairings were sparse. Scale bar represents 20 μm. (For interpretation of the references to colour in this figure legend, the reader is referred to the web version of this article.)

remodeling. Persistence of retinal output in RCS rats from 5 to 12 months has been confirmed with electrophysiological recordings from the optic tract (Cicerone, Green, & Fisher, 1979), the superior colliculus (Sauvé et al., 2001) and the visual cortex (Coffey et al., 2002; Girman, Wang, & Lund, 2003; Noell, Salinsky, Stockton, Schnitzer, & Kan, 1981). Noell et al. (1981) proposed that their cortical recordings reflected pure cone activity. Moreover, spectral sensitivity curves from optic tract recordings in albino RCS rats point to the likelihood that cone activity is the sole contributor to visual responsiveness in RCS rats aged from 150 to 300 days (Cicerone et al., 1979).

The histological preservation of rods and cones does not guarantee that these cells can generate a normal signal or that this signal can be appropriately processed by the downstream retinal circuitry. There are instances in which a certain treatment leads to morphological rescue that is not paralleled with functional rescue. The effect of HSV vector-delivered FGF2 on the light damaged RCS rat retina (Spencer, Agarwala, Gentry, & Brandt, 2001) and the effect of CNTF delivered by recombinant adeno-associated virus in the retina of mice with a P216L rds/peripherin mutation (Bok et al., 2002) are two examples. With this in mind, of particular relevance is the measure of rod and cone contribution to ERG responsiveness.

Our results show that following subretinal hSC injection, the mixed b-wave recorded at P60 is still largely driven by rod dependent activity. Although rod contribution to the b-wave diminishes with time, double flash-derived rod b-waves can still be recorded at P90, indicating that hSC injections do preserve some rod function. The observation that mixed scotopic responses can be elicited below cone threshold (-1.63 log cds/m^2 in non-dystrophics) gives additional support for the preservation of rod activity in hSC-injected rats. In untreated dystrophic RCS rats, not only are rod-driven b-waves no longer recorded by P90 but b-waves themselves can no longer be elicited (Pinilla et al., 2004). However, the rod b-waves rescued following subretinal hSC injection in dystrophic RCS rats saturate at lower flash intensities than in non-dystrophic RCS rats and plummet in amplitudes at higher intensities, suggesting that the rescued rods are more sensitive to light bleaching than in non-dystrophic rats. This finding is similar to the b-wave intensity responses recorded in albino rats where bright flashes bleach some of the visual pigment and deplete the enzyme phosphodiesterase, which normally provides a limiting step in the signal transduction cascade in response to high intensity flashes (Breton, Schueller, Lamb, & Pugh, 1994; Lyubarsky & Pugh, 1996) and is similar to our previous reports using hRPE for subretinal transplantation (Sauvé et al., 2006). Anatomically, about half the rods are preserved at P70 and the synaptic markers applied to the OPL showed apparently normal disposition of pre- and postsynaptic profiles associated with the rods. Nevertheless in addition

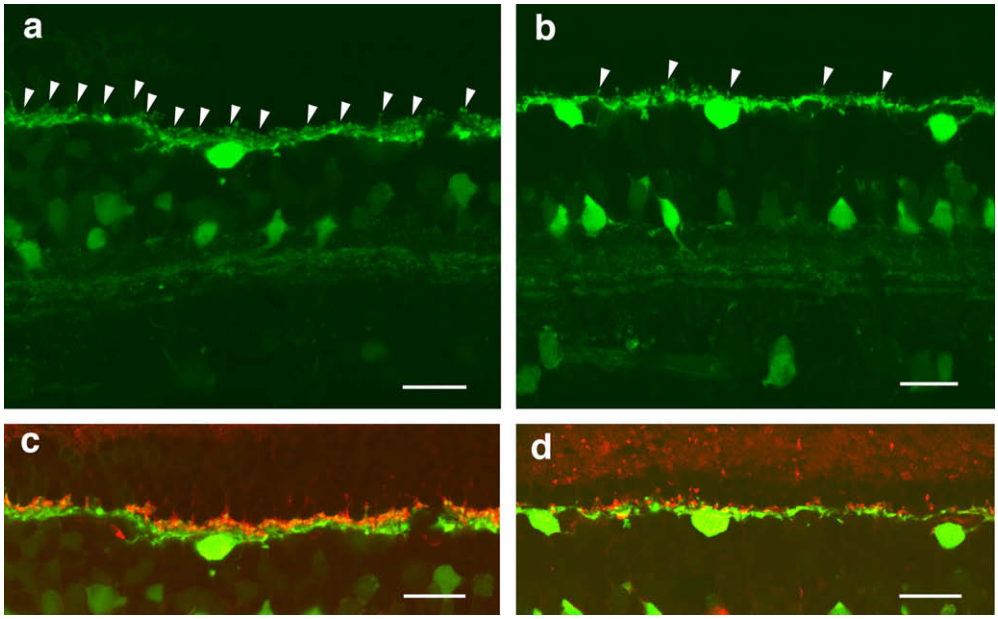

Fig. 9. Confocal fluorescence micrographs of retinal cross sections showing the preservation of horizontal cell terminals contacting photoreceptor axon terminals, using antibodies against calbindin (green) to label horizontal cells (a and b) and double immunostaining with antibodies to label photoreceptor terminals (synaptophysin, red channel) (c and d). In areas preserved by the transplant (a and c), horizontal cell terminal tips were well preserved (a, arrowheads) and synaptic contacts were clearly seen (c). Remote from the injection site, the horizontal cell terminals were sparse (b, arrowheads) and synaptophysin immunoreactivity was no longer distributed as a continuous layer and synaptic contacts were not maintained (d). Scale bar represents 20 μm. (For interpretation of the references to colour in this figure legend, the reader is referred to the web version of this article.)

to the abnormal ERG responses, light and dark adaptation studies, using multi-unit recordings defined visual receptive fields in the superior colliculus of RCS rats following preventive hSC injections, indicate that these animals are essentially "night blind" despite the persistence of rods up to 7 months of age (Girman et al., 2005). Therefore, although rod-driven activity can be recorded in retina, as indicated by full field ERG results, such information might not be processed appropriately at the CNS level. As seen with the hRPE transplantation, although Schwann cell injections sustain the synaptic connections made by rods in the outer plexiform layer, these do not guarantee normal rod function. Phototransduction may still be compromised and this could be the reason of the changes in the ERG response. However it is also possible that since the grafted cells do not protect the whole area of the retina, the dystrophic region distant from the grafted cells could influence the full-field ERG response.

Subretinal hSC injections also lead to the preservation of cone function. Isolated cone b-waves do not show signs of bleaching as in sham-injected rats, neither under scotopic nor under photopic adaptation. Intensity response curves for isolated scotopic cone b-waves are similar to those for photopic b-waves, suggesting that the double flash protocol used here is reliable in extracting the cone-driven contribution from the mixed scotopic ERG. Preservation of cone function is confirmed by flicker responsiveness. Both maximal amplitudes and flicker fusion are significantly higher in hSC-injected compared with sham-injected eyes at P60. However, there is an obvious deterioration in cone responses with age. Other tests, applied in the same therapeutic model, have shown that cone function can persist much longer than suggested by ERG results: (1) lower visual thresholds at P180 as indicated by superior colliculus recordings under mesopic conditions (Sauvé et al., 2002); (2) higher acuity as measured behaviorally under photopic conditions (McGill et al., 2004); and (3) preserved responsiveness of well tuned single unit responses in the primary visual cortex, also under photopic conditions (Girman et al., 2003).

A unique characteristic of the sham-injected eyes is the occurrence, both under scotopic and photopic adaptation, of a high threshold STR-like negative component at P60. In hSC-injected animals such negative waves were never seen (data not shown). A similar STR-like component has been reported in aged RCS rats, both under scotopic (Bush et al., 1995) and photopic (Sugawara, Machida, Sieving, & Bush, 1999) conditions, at a time when no other components can be elicited. The negative STR-like wave effectively reduces the b-wave amplitude. Intravitreal injections of NMA (N-methyl-D, L-aspartic acid), which blocks activity from third order neurons, increase the b-wave in 10 weeks old RCS rats, suggesting that a negative STR-like component (driven by third order neurons) is superimposed on the positive b-wave (Machida, Raz-Prag, Fariss, Sieving, & Bush, 2008). Similar unmasking effects were obtained here using the double flash approach, suggesting that STR-like generators can be bleached or saturated at advanced degenerative stages. Studies of dynamic of recovery from conditioning flash indicate that unmasking (seen as an "overshooting" from normalized responses) was maximal at 120 ms intervals. The fact that "overshooting" was exacerbated in sham-injected animals indicates that the STR-like negative wave constituted a larger proportion of the mixed responses than in hSC-injected animals. It is possible that this STR-like wave might reflect the activity from intrinsically photosensitive RGCs that are adapting to light (Wong, Dunn, & Berson, 2004). However, if STR-like responses are indeed a reflection of melanopsin-dependent phototransduction, then the STR would not be expected to be normal since melanopsin mRNA levels have been shown to be severely decreased by P60 in RCS rats (Sakamoto, Liu, & Tosini, 2004). It remains possible that preventive therapy might preserve this component, and that a larger amplitude STR might serve as an indicator of functional preservation in degenerative stages for which b-waves cannot be elicited (Vollrath et al., 2001).

A number of different cell types have shown to be effective in preserving morphological and functional characteristics in the dystrophic RCS rats. While previous studies have not examined the effects on the electroretinogram responses in such detail, the general principle emerges that cells such as Schwann cells, that most likely function by delivery of growth factors provide very similar results

to retinal pigment epithelial cells, which appear to function by replacing some at least of the RPE functions essential for photoreceptor survival. Another cell type of mixed function, a human neural progenitor cell delivers among the best and longest preservation, when evaluated using ERG, behavior test and immunohistochemistry (Gamm et al., 2007; Lund et al., 2006; Lund, Wang, Lu, Girman, Holmes, Sauvé, et al., 2006). With time and in the non preserved areas, the debris zone appeared again in almost all the cell types that our group had studied. It should be noted however that some cells, including fibroblasts and placental-derived cells (Lund et al., 2006) fail to support photoreceptor survival, indicating that the effect is not simply a non-specific effect of introducing cells to the subretinal space of RCS rats.

It is not clear which factors might be responsible for the survival effect seen with Schwann cells, although a study using rat-derived Schwann cell lines, in which the native cell was ineffective in rescuing photoreceptors, showed that GDNF-secreting cells were very effective in prmoting rescue, and that BDNF cells appeared to give some level of protection over background. One relevant issue in the present study is that while such factors may have effects beyond photoreceptor survival, the Schwann cell transplants do not appear to have extraneous or deleterious effects on retinal morphology or function (Lawrence et al., 2004).

In summary, this study reports the detailed ERG changes encountered with photoreceptor rescue achieved by introduction of a cell type (Schwann cell) that functions mostly likely by releasing a range of neuroprotective factors. It is remains, however, that retinal physiology is not fully restored by this therapeutic approach, despite the relatively normal appearing outer retina morphology and the results of previous studies showing good rescue of visual behavioral responses. These observations point to some level of phototransduction dysfunction that has not been corrected by the treatment and the possibility that gain changes in the relay of the visual signals through the various layers of the retina and CNS might partially compensate for some pathological changes that could not be prevented by Schwann cell injection.

Acknowledgments

The authors would like to thank Dr. S. Wang for preparing the human Schwann cells and Dr. B. Lu for injecting them in the subretinal space of RCS rats.

References

Arnhold, S., Heiduschka, P., Klein, H., Absenger, Y., Basnaoglu, S., Kreppel, F., et al. (2006). Adenovirally transduced bone marrow stromal cells differentiate into pigment epithelial cells and induce rescue effects in RCS rats. *Investigative Ophthalmology Visual Science, 47*, 4121–4129.

Bok, D., Yasumura, D., Matthes, M. T., Ruiz, A., Duncan, J. L., Chappelow, A. V., et al. (2002). Effects of adeno-associated virus-vectored ciliary neurotrophic factor on retinal structure and function in mice with a P216L rds/peripherin mutation. *Experimental Eye Research, 74*, 719–735.

Bourne, M. C., Campbell, D. A., & Tansley, K. (1938). Hereditary degeneration of the rat retina. *British Journal Ophthalmology, 22*(10), 613–623.

Breton, M. E., Schueller, A. W., Lamb, T. D., & Pugh, E. N. Jr., (1994). Analysis of ERG a-wave amplification and kinetics in terms of the G-protein cascade of phototransduction. *Investigative Ophthalmology Visual Science, 35*(1), 295–309.

Bush, R. A., Hawk, K. W., & Sieving, P. A. (1995). Preservation of inner retinal responses in the Aged royal college of surgeons rat. Evidence against glutamate excitotoxicity in photoreceptor degeneration. *Investigative Ophthalmology Visual Science, 36*, 2054–2062.

Cayouette, M., Behn, D., Sendtner, M., Lachapelle, P., & Gravel, C. (1998). Intraocular gene transfer of ciliary neurotrophic factor prevents death and increases responsiveness of rod photoreceptors in the retinal degeneration slow mouse. *Journal of Neuroscience, 18*(22), 9282–9293.

Cicerone, C. M., Green, D. G., & Fisher, L. J. (1979). Cone inputs to ganglion cells in hereditary retinal degeneration. *Science, 203*(4385), 1113–1115.

Coffey, P. J., Girman, S., Wang, S. M., Hetherington, L., Keegan, D. J., Adamson, P., et al. (2002). Long-term preservation of cortically dependent visual function in RCS rats by transplantation. *Nature Neuroscience, 5*, 53–56.

Cotter, J. R., & Noell, W. K. (1984). Ultrastructure of remnant photoreceptors in advanced hereditary retinal degeneration. *Investigative Ophthalmology Visual Science, 25*, 1366–1375.

Cuenca, N., Pinilla, I., Sauvé, Y., Lu, B., Wang, S., & Lund, R. D. (2004). Regressive and reactive changes in the connectivity patterns of rod and cone pathways of P23H transgenic rat retina. *Neuroscience, 127*(2), 301–317.

Cuenca, N., Pinilla, I., Sauvé, Y., & Lund, R. D. (2005). Early changes in synaptic connectivity following progressive photoreceptor degeneration in RCS rats. *European Journal of Neuroscience, 22*(5), 1057–1072.

Davidorf, F. H., Mendlovic, D. B., Bowyer, D. W., Gresak, P. M., Foreman, B. C., Werling, K. T., et al. (1991). Pathogenesis of retinal dystrophy in the royal college of surgeons rat. *Annals of Ophthalmolology, 23*(3), 87–94.

D'Cruz, P. M., Yasumura, D., Weir, J., Matthes, M. T., Abderrahim, H., LaVail, M. M., et al. (2000). Mutation of the receptor tyrosine kinase gene Mertk in the retinal dystrophic RCS rat. *Human Molecular Genetics, 9*, 645–651.

Dowling, J. E., & Sidman, R. L. (1962). Inherited retinal dystrophy in the rat. *Journal of Cell Biology, 14*, 73–109.

Gal, A., Li, Y., Thompson, D. A., Weir, J., Orth, U., Jacobson, S. G., et al. (2000). Mutations in MERTK, the human orthologue of the RCS rat retinal dystrophy gene, cause retinitis pigmentosa. *Nature Genetics, 26*, 270–271.

Gamm, D. M., Wang, S., Lu, B., Girman, S., Holmes, T., Bischoff, N., et al. (2007). Protection of visual functions by human neural progenitors in a rat model of retinal disease. *PLoS ONE, 28*(2), e338.

Girman, S. V., Wang, S., & Lund, R. D. (2003). Cortical visual functions can be preserved by subretinal RPE cell grafting in RCS rats. *Vision Research, 43*, 1817–1827.

Girman, S. V., Wang, S., & Lund, R. D. (2005). Time course of deterioration of rod and cone function in RCS rat and the effects of subretinal cell grafting: A light- and dark-adaptation study. *Vision Research, 45*(3), 343–354.

Gu, S. M., Thompson, D. A., Srikumari, C. R., Lorenz, B., Finckh, U., Nicoletti, A., et al. (1997). Mutation in RPE65 cause autosomal recessive childhood-onset severe retinal dystrophy. *Nature Genetics, 17*, 194–197.

Hammarberg, H., Piehl, F., Cullheim, S., Fjell, J., Hökfelt, T., & Fried, K. (1996). GDNF mRNA in Schwann cells and DRG satellite cells after chronic sciatic nerve injury. *Neuroreport, 7*(4), 857–860.

Hattar, S., Liao, H. W., Takao, M., Berson, D. M., & Yau, K. W. (2002). Melanopsin-containing retinal ganglion cells: Architecture, projections, and intrinsic photosensitivity. *Science, 295*, 1065–1070.

Huang, Q., Xu, P., Xia, X., Hu, H. H., Wang, F., & Li, H. M. (2006). Subretinal transplantation of human fetal lung fibroblasts expressed ciliary neurotrophic factor gene prevent photoreceptor degeneration in RCS rats. *Zhonghua Yan Ke Za Zhi, 42*, 127–130.

Inoue, Y., Iriyama, A., Ueno, S., Takahashi, H., Kondo, M., Tamaki, Y., et al. (2007). Subretinal transplantation of bone marrow mesenchymal stem cells delays retinal degeneration in the RCS rat model of retinal degeneration. *Experimental Eye Research, 85*, 234–241.

Keegan, D. J., Kenna, P., Humphries, M. M., Humphries, P., Flitcroft, D. I., Coffey, P. J., et al. (2003). Transplantation of syngeneic Schwann cells to the retina of the rhodopsin knockout (rho(−/−)) mouse. *Investigative Ophthalmology Visual Science, 44*(8), 3526–3532.

LaVail, M. M., Sidman, R. L., & Gerhardt, C. O. (1975). Congenic strains of RCS rats with inherited retinal dystrophy. *The Journal of Heredity, 66*, 242–244.

LaVail, M. M., Sidman, M., Rausin, R., & Sidman, R. L. (1974). Discrimination of light intensity by rats with inherited retinal degeneration: A behavioral and cytological study. *Vision Research, 14*, 693–702.

Lawrence, J. M., Keegan, D. J., Muir, E. M., Coffey, P. J., Rogers, J. H., Wilby, M. J., et al. (2004). Transplantation of Schwann cell line clones secreting GDNF or BDNF into the retinas of dystrophic royal college of surgeons rats. *Investigative Ophthalmology Visual Science, 45*(1), 267–274.

Lawrence, J. M., Sauvé, Y., Keegan, D. J., Coffey, P. J., Hetherington, L., Girman, S., et al. (2000). Schwann cell grafting into the retina of the dystrophic RCS rat limits functional deterioration. Royal college of surgeons. *Investigative Ophthalmology Visual Science, 41*(2), 518–528.

Lin, N., Fan, W., Sheedlo, H. J., Aschenbrenner, J. E., & Turner, J. E. (1996). Photoreceptor repair in response to RPE transplants in RCS rats: Outer segment regeneration. *Current Eye Research, 15*, 1069–1077.

Little, C. W., Castillo, B., DiLoreto, D. A., Cox, C., Wyatt, J., del Cerro, C., et al. (1996). Transplantation of human fetal retinal pigment epithelium rescues photoreceptor cells from degeneration in the royal college of surgeons rat retina. *Investigative Ophthalmology Visual Science, 37*, 204–211.

Lund, R. D., Adamson, P., Sauve, Y., Keegan, D. J., Girman, S. V., Wang, S., et al. (2001). Subretinal transplantation of genetically modified human cell lines attenuates loss of visual function in dystrophic rats. *Proceedings of the National Academy of Sciences of the United States of America, 98*, 9942–9947.

Lund, R. D., Wang, S., Klimanskaya, I., Holmes, T., & Ramos-Kelsey, R. (2006). Human embryonic stem cell-derived cells rescue visual function in dystrophic RCS rats. *Cloning Stem Cells, 8*, 189–199.

Lund, R. D., Wang, S., Lu, B., Girman, S., Holmes, T., Sauvé, Y., et al. (2006). Cells isolated from umbilical cord tissue rescue photoreceptors and visual functions in a rodent model of retinal disease. *Stem Cells, 25*, 602–611.

Lyubarsky, A. L., & Pugh, E. N. Jr., (1996). Recovery phase of the murine rod photoresponse reconstructed from electroretinographic recordings. *Journal of Neuroscience, 16*, 563–571.

Machida, S., Raz-Prag, D., Fariss, R. N., Sieving, P. A., & Bush, R. A. (2008). Photopic ERG negative response from amacrine cell signaling in RCS rat retinal degeneration. *Investigative Ophthalmology Visual Science, 49*, 442–452.

Marlhens, F., Bareil, C., Griffoin, J. M., Zrenner, E., Amalric, P., Eliaou, C., et al. (1997). Mutation in RPE65 cause Leber's congenital amaurosis. *Nature Genetics, 17*, 139–141.

Maw, M. A., Kennedy, B., Knight, A., Bridges, R., Roth, K. E., Mani, E. J., et al. (1997). Mutation of the gene encoding cellular retinal–aldehyde–binding protein in autosomal recessive retinitis pigmentosa. *Nature Genetics, 17*, 198–200.

McGill, T. J., Douglas, R. M., Lund, R. D., & Prusky, G. T. (2004). Quantification of spatial vision in the royal college of surgeons rat. *Investigative Ophthalmology Visual Science, 45*, 932–936.

McGill, T. J., Lund, R. D., Douglas, R. M., Wang, S., Lu, B., & Prusky, G. T. (2004). Preservation of vision following cell-based therapies in a model of retinal degenerative disease. *Vision Research, 44*, 2559–2566.

McHenry, C. L., Liu, Y., Feng, W., Nair, A. R., Feathers, K. L., Ding, X., et al. (2004). MERTK arginine-844-cysteine in a patient with severe rod-cone dystrophy: Loss of mutant protein function in transfected cells. *Investigative Ophthalmology Visual Science, 45*, 1456–1463.

Meyer, M., Matsuoka, I., Wetmore, C., Olson, L., & Thoenen, H. (1992). Enhanced synthesis of brain-derived neurotrophic factor in the lesioned peripheral nerve: Different mechanisms are responsible for the regulation of BDNF and NGF mRNA. *Journal of Cell Biology, 119*(1), 45–54.

Mirshahi, M., Thillaye, B., Tarraf, M., de Kozak, Y., & Faure, J. P. (1994). Light-induced changes in S-antigen (arrestin) localization in retinal photoreceptors: Differences between rods and cones and defective process in RCS rat retinal dystrophy. *European Journal of Cell Biology, 63*(1), 61–67.

Mizumoto, H., Mizumoto, K., Shatos, M. A., Klassen, H., & Young, M. J. (2003). Retinal transplantation of neural progenitor cells derived from the brain of GFP transgenic mice. *Vision Research, 43*, 1699–1708.

Nandrot, E., Dufour, E. M., Provost, A. C., Pequignot, M. O., Bonnel, S., Gogat, K., et al. (2000). Homozygous deletion in the coding sequence of the c-mer gene in RCS rats unravels general mechanisms of physiological cell adhesion and apoptosis. *Neurobiology Diseases, 7*, 586–599.

Neuberger, T. J., & De Vries, G. H. (1993). Distribution of fibroblast growth factor in cultured dorsal root ganglion neurons and Schwann cells. II. Redistribution after neural injury. *Journal of Neurocytology, 22*, 449–460.

Noell, W. K., Salinsky, M. C., Stockton, R. A., Schnitzer, S. B., & Kan, V. (1981). Electrophysiological studies of the visual capacities at advanced stages of photoreceptor degeneration in the rat. *Documenta ophthalmologica. Proceedings series, 27*, 175.

Ohguro, H., Ohguro, I., Mamiya, K., Maeda, T., & Nakazawa, M. (2003). Prolonged survival of the phosphorylated form of rhodopsin during dark adaptation of royal college surgeons rat. *FEBS Letters, 551*(1–3), 128–132.

Peng, Y. W., Senda, T., Hao, Y., Matsuno, K., & Wong, F. (2003). Ectopic synaptogenesis during retinal degeneration in the royal college of surgeons rat. *Neuroscience, 119*, 813–820.

Petrukhin, K., Koisti, M. J., Bakall, B., Li, W., Xie, G., Marknell, T., et al. (1998). Identification of the gene responsible for Best macular dystrophy. *Nature Genetics, 19*, 241–247.

Pinilla, I., Cuenca, N., Sauvé, Y., Wang, S., & Lund, R. D. (2007). Preservation of outer retina and its synaptic connectivity following subretinal injections of human RPE cells in the royal college of surgeons rat. *Experimental Eye Research, 85*(3), 381–392.

Pinilla, I., Sauvé, Y., & Lund, R. D. (2004). Contribution of rod and cone pathways to dark-adapted electroretinogram (ERG) b-wave following retinal degeneration in RCS rats. *Vision Research, 44*, 2467–2474.

Pinilla, I., Sauvé, Y., & Lund, R. D. (2005). Cone function studied with flicker electroretinogram during progressive retinal degeneration in RCS rats. *Experimental Eye Research, 80*(1), 51–59.

Rezai, K. A., Kohen, L., Wiedemann, P., & Heimann, K. (1997). Iris pigment epithelium transplantation. *Graefe's Archive for Clinical and Experimental Ophthalmology, 235*, 558–562.

Sakamoto, K., Liu, C., & Tosini, G. (2004). Classical photoreceptors regulate melanopsin mRNA levels in the rat retina. *Journal of Neuroscience, 24*, 9693–9697.

Sauvé, Y., Girman, S. V., Wang, S., Keegan, D. J., & Lund, R. D. (2002). Preservation of visual responsiveness in the superior colliculus of RCS rats after retinal pigment epithelium cell transplantation. *Neuroscience, 114*, 389–401.

Sauvé, Y., Girman, S. V., Wang, S., Lawrence, J. M., & Lund, R. D. (2001). Progressive visual sensitivity loss in the royal college of surgeons rat: Perimetric study in the superior colliculus. *Neuroscience, 103*, 51–63.

Sauvé, Y., Klassen, H., Whiteley, S. J., & Lund, R. D. (1998). Visual field loss in RCS rats and the effect of RPE cell transplantation. *Experimental Neurology, 152*, 243–250.

Sauvé, Y., Lu, B., & Lund, R. D. (2004). The relationship between full field electroretinogram and perimetry-like visual thresholds in RCS rats during photoreceptor degeneration and rescue by cell transplants. *Vision Research, 44*, 9–18.

Sauvé, Y., Pinilla, I., & Lund, R. D. (2006). Partial preservation of rod and cone ERG function following subretinal injection of ARPE-19 cells in RCS rats. *Vision Research, 46*(8–9), 1459–1472.

Schraermeyer, U., Kociok, N., & Heimann, K. (1999). Rescue effects of IPE transplants in RCS rats: Short-term results. *Investigative Ophthalmology Visual Science, 40*, 1545–1556.

Schraermeyer, U., Thumann, G., Luther, T., Kociok, N., Armhold, S., Kruttwig, K., et al. (2001). Subretinally transplanted embryonic stem cells rescue photoreceptor cells from degeneration in the RCS rats. *Cell Transplantation, 10*, 673–680.

Seiler, M. J., Sagdullaev, B. T., Woch, G., Thomas, B. B., & Aramant, R. B. (2005). Transsynaptic virus tracing from host brain to subretinal transplants. *European Journal of Neuroscience, 21*, 161–172.

Sendtner, M., Stöckli, K. A., & Thoenen, H. (1992). Synthesis and localization of ciliary neurotrophic factor in the sciatic nerve of the adult rat after lesion and during regeneration. *Journal of Cell Biology, 118*(1), 139–148.

Spencer, B., Agarwala, S., Gentry, L., & Brandt, C. R. (2001). HSV-1 vector-delivered FGF2 to the retina is neuroprotective but does not preserve functional responses. *Molecular Therapy, 3*, 746–756.

Sugawara, T., Machida, S., Sieving, P.A., & Bush, R.A. (1999). The photopic ERG of the light damaged and RCS rat: Persistence of a nagative component from the inner retina. *Investigative Ophthalmology Visual Science*, *40*(4), S23, Abstract 118.

Thompson, D. A., McHenry, C. L., Li, Y., Richards, J. E., Othman, M. I., Schwinger, E., et al. (2002). Retinal dystrophy due to paternal isodisomy for chromosome 1 or chromosome 2, with homoallelism for mutations in RPE65 or MERTK, respectively. *American Journal Human Genetics, 70*, 224–229.

Thumann, G., Salz, A. K., Walter, P., & Johnen, S. (2009). Preservation of photoreceptors in dystrophic RCS rats following allo- and xenotransplantation of IPE cells. *Graefe's Archive for Clinical and Experimental Ophthalmology, 247*, 363–369.

Vollrath, D., Feng, W., Duncan, J. L., Yasumura, D., D'Cruz, P. M., Chappelow, A., et al. (2001). Correction of the retinal dystrophy phenotype of the RCS rat by viral gene transfer of Mertk. *Proceedings of the National Academy of Sciences of USA, 98*, 12584–12589.

Wang, S., Lu, B., Wood, P., & Lund, D. (2005). Distribution over time of ARPE-19 and Schwann Cells after Grafting to the Subretinal Space in RCS Rats and the Relation to Photoreceptor Rescue. *Investigative Ophthalmology Visual Science, 46*, 2552–2560.

Wang, S., Lu, B., & Lund, R. D. (2005). Morphological changes in the royal college of surgeons rat retina during photoreceptor degeneration and after cell-based therapy. *Journal of Comparative Neurology, 491*(4), 400–417.

Wojciechowski, A. B., Englund, U., Lundberg, C., Wictorin, K., & Warfvinge, K. (2002). Subretinal transplantation of brain-derived precursor cells to young RCS rats promotes photoreceptor cell survival. *Experimental Eye Research, 75*, 23–37.

Wong, K. Y., Dunn, F. A., Berson, D. M. (2004). *Adaptation in ganglion-cell photoreceptors*, Society Neuroscience Abstract 750.7.